Breathing-In/Breathing-Out Approach to Preparing Nanosilver-Loaded Hydrogels: Highly Efficient Antibacterial Nanocomposites

Varsha Thomas,[1] Murali Mohan Yallapu,[2]* B. Sreedhar,[3] S. K. Bajpai[1]

[1]*Department of Chemistry, Polymer Research Laboratory, Government Model Science College, Jabalpur, MP 482001, India*
[2]*Department of Polymer Science and Technology, Sri Krishnadevaraya University, Anantapur, AP 515003, India*
[3]*Inorganic and Physical Chemistry, Indian Institute of Chemical Technology, Tarnaka, Hyderabad, AP 500007, India*

Received 22 January 2008; accepted 5 July 2008
DOI 10.1002/app.29018
Published online 17 October 2008 in Wiley InterScience (www.interscience.wiley.com).

ABSTRACT: The key objective of developing novel materials for hygienic living conditions is to lower the risk of transmitting diseases and biofouling. To this end, a number of silver–hydrogel nanocomposite systems are under development. In this study, we attempted a unique strategy to prepare silver-nanoparticle-loaded poly(acrylamide-*co*-*N*-vinyl-2-pyrolidone) hydrogel composites. To load nanosilver particles into such a nonionic hydrogel, a novel breathing-in/breathing-out (BI–BO) approach was employed. As the number of BI–BO cycles increased, the amount of the silver nanoparticles loaded into these hydrogels also increased. This behavior was obvious and was confirmed by ultraviolet–visible spectroscopy and thermal analysis. Furthermore, the hydrogel–silver-nanoparticle composites were confirmed with Fourier transform infrared spectroscopy and transmission electron microscopy studies. Antibacterial studies of these hydrogel–silver nanocomposites showed excellent results against *Escherichia coli*. The antibacterial activity increased with the number of BI–BO cycles, and samples that underwent three BI–BO cycles showed optimal bactericidal activity. The degree of crosslinking and the silver content had a great influence on the antibacterial efficacy. J Appl Polym Sci 111: 934–944, 2009

Key words: biological applications of polymers; nanocomposites; swelling; TEM; UV-vis spectroscopy

INTRODUCTION

Among inorganic antibacterial agents, silver has been identified as a material extensively studied since ancient times to fight infections and control spoilage.[1] The antibacterial and antiviral actions of silver, silver ions, and silver compounds have been thoroughly investigated.[2–8] Silver nanoparticles have opened a new era in the fight against diseases such as methicillin-resistant *Staphylococcus aureus*, cystic fibrosis, and acquired immune deficiency syndrome and in the treatment of wounds (http://www.oaresearch.co.uk/pressrelease.pdf). The profound activity of silver nanoparticles is due to their high surface area to volume ratios and crystallographic surface structural features. A study by Morones et al.[9] demonstrated that the bactericidal activities of silver nanoparticles are size-dependent. It is very clear that silver nanoparticles are small enough to pass through the outer cell membranes, enter the cells by inner mechanisms, and damage the cells. A recent investigation reported that silver nanoparticles with three different capping agents, such as foamy carbon, poly(vinyl pyrrolidone), and bovine serum albumin, exhibited toxicity toward human immunodeficiency virus 1 cells.[10] The proposed mechanism is that the nanoparticles bind to the gp120 glycoprotein knobs of human immunodeficiency virus 1 by using the sulfur residues on the knobs. The silver nanoparticles ($\sim$ 10 nm) easily penetrate the cells, which have a spacing between the knobs of $\sim$ 22 nm. Thus, nanosilver has been used in a wide range of healthcare products, such as burn dressings, scaffolds at skin donor and recipient sites, water purification systems, and medical devices.[11,12]

Recently, polymer scientists have focused on the development of polymer–nanosilver materials that exhibit antimicrobial properties. The reason behind these continuous efforts is that such antimicrobial polymers, when coated onto the surfaces of various medical devices such as urinary catheters, cannulae,

Additional Supporting Information may be found in the online version of this article.

**Present address:* Department of Biomedical Engineering ND-20, Lerner Research Institute, Cleveland Clinic Foundation, Cleveland, OH 44195.

Correspondence to: S. K. Bajpai (mnlbpi@rediffmail.com).

surgical gloves, and dressing materials, prevent bacterial infections.[13–16] Yu et al.[16] prepared poly(vinyl pyrrolidone)–poly(vinyl alcohol) hydrogels containing 20–100-nm silver nanoparticles by a repeated freezing–thawing treatment and investigated their antibacterial properties against *Escherichia coli*. They reported that the freezing–thawing treatment resulted in the formation of three-dimensional structures, and no serious aggregation of silver nanoparticles occurred. These nanosilver-containing hydrogels showed excellent antibacterial effect. Likewise, Lee and Huang[17] prepared a series of antibacterial superabsorbents containing silver nanoparticles that were based on sodium acrylate, a 1-vinyl-2-pyrrolidone–silver-ion complex, and *N,N′*-methylene bisacrylamide (MBA) by inverse suspension polymerization. Ascorbic acid was used as a reductant to reduce the silver-ion complex in gel through an *in situ* reduction method. They also showed the reflective antibacterial activity of superabsorbents against *Candida albicans* with an increase in the silver concentration (1–10 ppm).

A few trends based on hydrogel–silver nanocomposite systems have revealed outstanding antibacterial properties. The three-dimensional networks of hydrogels provide enough space for nucleation and growth of nanoparticles and are of biomedical interest because of their compatibility with biological molecules, cells, tissues, and so forth.[18–20] Zhang et al.[21] produced polymeric microgels to act as versatile nanoreactors for developing semiconductor, metal, and magnetic nanoparticles. Silver nanoparticles $\sim$ 35 nm in size, embedded in a novel hydrogel system based on poly(vinyl alcohol)/polystyrene-*co*-poly (ethylene glycol dimethacrylate), have been developed.[22] Another study has demonstrate that hydrogels are also effective in producing nanosized silver particles ($\sim$ 4 nm).[23] Mohan et al.[24] grew silver nanoparticles inside poly(*N*-isopropylacrylamide-*co*-sodium acrylate) hydrogel networks. Quite recently, we reported a unique approach to incorporating nanosilver into poly(acrylamide-*co*-acrylic acid) hydrogels[25] and also investigated the biocidal action of the resulting material. This approach involved the immersion of a swollen hydrogel in a silver nitrate ($AgNO_3$) aqueous solution to induce ion exchange between Ag^+ ions of the solution and H^+ ions present in the swollen hydrogel network, followed by citrate reduction. However, this approach cannot be applied to incorporating Ag^+ ions into polymer networks composed of nonionic monomers. Therefore, to prepare a silver-nanoparticle-containing polymeric hydrogel with neutral monomers as repeat units, we report a unique breathing-in/breathing-out (BI–BO) method for the synthesis of nanosilver-loaded poly (acrylamide-*co*-*N*-vinyl-2-pyrrolidone) hydrogels. When a shrunken gel is placed in an aqueous solution of silver nanoparticles, it undergoes appreciable swelling by absorbing the surrounding aqueous medium. The absorption of the aqueous medium by the gel may be considered a breathing-in process. Later on, when the swollen gel is put in acetone, the gel undergoes drastic deswelling by expelling water. The expulsion of water from the swollen gel network may be considered a breathing-out process. This swelling–shrinking behavior of gels has been exploited to introduce silver nanoparticles into gels. Finally, the resultant nanosilver-containing gels have also been investigated for antibacterial properties against *E. coli*.

EXPERIMENTAL

Materials

The two monomers used in this study, acrylamide (AAm) and *N*-vinyl-2-pyrrolidone (NVP), and the crosslinking agent MBA were obtained from HiMedia Laboratories (Mumbai, India). $AgNO_3$, trisodium citrate, acetone, and potassium persulfate (KPS) were obtained from E. Merck (Mumbai, India) and used as received. Standard cultures of the organisms were provided by the Department of Biotechnology, Government Model Science College (Jabalpur, India). Nutrient broth and nutrient and m-endo agars were obtained from HiMedia Chemicals (Mumbai, India). Double-distilled water (18 mΩ) was used throughout the investigation.

Synthesis of the silver nanoparticles

Silver nitrate (0.24×10^{-3} *M*) was dissolved in a 50-mL aqueous solution of aqueous 1% trisodium citrate (w/v) and kept at room temperature. The progress of the formation of silver nanoparticles was monitored by the measurement of the surface plasmon resonance of the solution at different time intervals with a Shimadzu (Japan) UV1700 ultraviolet–visible (UV–vis) spectrophotometer, and the size was measured with a Mastersizer 2000 (version 2.00, Malvern, United Kingdom; see the supporting information).

Synthesis of the hydrogels

The hydrogel discs were prepared through the free-radical aqueous copolymerization of AAm and NVP in the presence of the MBA crosslinker with KPS as the initiator. In a typical procedure, 14.08 m*M* AAm, 8.99 m*M* NVP, and 0.32 m*M* MBA were dissolved in water, and the final volume was made up to 5 mL. Then, 0.11 m*M* KPS was added, and the whole reaction mixture was transferred to a test tube (internal diameter = 1.5 cm) and kept in an electric oven (Tempstar, New Delhi, India) at 60°C for a period of

TABLE I
Compositions of Various Copolymeric Hydrogels

Sample	Concentrations in the feed mixture			
	AAm (mM)	NVP (mM)	MBA (mM)	KPS (mM)
HGA	14.08	8.99	0.13	0.11
HGB	14.08	8.99	0.26	0.11
HGC	14.08	8.99	0.45	0.11
HGD	14.08	8.99	0.64	0.11

2 h. After the polymerization was over, the test tube was broken, and the resultant transparent hydrogels were cut into slices about 3 mm thick. The hydrogels were equilibrated in distilled water for a period of 2 days to remove the unreacted salts and finally dried in a dust-free vacuum chamber until the gels attained a constant weight. In a similar way, different samples were prepared by changes in the monomer and crosslinker concentrations, and the complete compositions are given in Table I.

Swelling and deswelling studies

A completely dried and preweighed hydrogel disc was placed in 250 mL of distilled water at 27 ± 0.2°C, and its water uptake was measured periodically by removal of the gel, blotting of excess water on the surface of the gel, and weighing with an analytical balance (K. Roy and Co., New Delhi, India) with a precision of 0.0002 g. For deswelling (shrinking) studies, completely swollen discs were placed in 30 mL of acetone, and the water loss from the gel was measured periodically by removal of the gel from acetone, blotting of excess acetone on the surface of the gel, and weighing with an analytical balance. The mass swelling percentage was determined as follows:

$$\text{Swelling}(\%) = [(w_t - W_0)/W_0] \times 100$$

where W_t and W_0 are the weights of the gel at time t and in its dry state, respectively. All the swelling and deswelling experiments were carried out in triplicate, and average values are presented in the data.

Incorporation of the silver nanoparticles into the hydrogels

The silver nanoparticles were loaded into the swollen gel with the newly developed BI–BO approach at 27 ± 0.2°C. The swollen disc was placed in 30 mL of acetone for a period of 2 h to obtain a shrunken gel, which was then put into 100 mL of a citrate-stabilized silver-nanoparticle solution for 24 h to allow the silver nanoparticles into the swelling gel disc. Then, the nanosilver-containing swollen gel was again put in acetone for dewatering, which resulted in a dark brown disc; this indicated the presence of the nanoparticles.

Characterization

The thermal history of the hydrogel and nanosilver-loaded hydrogels were evaluated on a DuPont (Japan) 2100 thermogravimetric analysis (TGA) instrument at a heating rate of 10°C/min under a 50 mL/min nitrogen flow. Dry samples, with a weight of 9.2 mg each, were heated from room temperature to 900°C. Each TGA was repeated four times, and averages and standard deviations are reported. The Fourier transform infrared spectra of the plain and silver-nanoparticle-loaded hydrogel samples were recorded on a Shimadzu 8400 S Fourier transform infrared spectrophotometer using KBr. The spectra exhibited a characteristic peak for N—H stretching of the amide at 3667 cm^{-1}. Asymmetric C—H stretching was obtained at 3000–2800 cm^{-1}, whereas symmetric C—H stretching was obtained in the range of 2500–2000 cm^{-1}. The medium peak in the region of 1500–1445 cm^{-1} was due to C—H bending. The medium peak at 1350–1010 cm^{-1} was due to the C—N group of the aliphatic and aromatic amines of VP.

An Escalab (Japan) X-ray photoelectron spectroscopy apparatus (Mg Kα, $h\nu = 1253.6$ eV) with a resolution of 1.0×10^{-4} Pa was used to confirm the formation of the silver nanoparticles.

Transmission electron microscopy (TEM) images of the samples were recorded with a Tecnai F 12 TEM instrument (Japan). To prepare samples for TEM analysis, a silver-loaded hydrogel was ground in a ball mill, and then a definite quantity of the ground powder was dispersed in distilled water and finally equilibrated for at least 7 days. This process allowed some loaded particles to come out of the hydrogel matrix. Now, two or three drops of the gel–silver-nanoparticle composite solution were dispersed on a 200-mesh formvar-coated copper grid (97 μm) and dried at room temperature after the removal of excess solution with filter paper.

Microbial experimentation

Microbial experimentation was performed to determine the effect of the silver–hydrogel composite on the Gram-negative bacteria *E. coli*. For this purpose, approximately 10^8 CFU of *E. coli* was cultured on nutrient agar plates supplemented with a calculated amount of nanosilver-loaded hydrogel particles (size = 211 μm). Plain hydrogels were used as controls. The plates were incubated for 24 h at 37°C, and the number of colonies was counted.

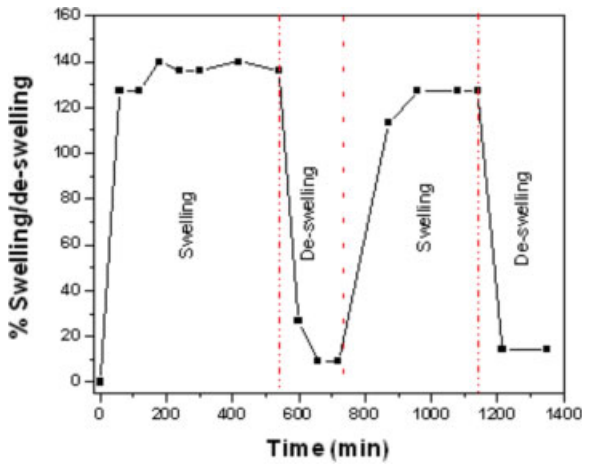

Figure 1 Graph showing the swelling–deswelling cycle of sample HGD. [Color figure can be viewed in the online issue, which is available at www.interscience.wiley.com.]

RESULTS AND DISCUSSION

Swelling–shrinking behavior of the hydrogels

The maintenance of the structural integrity of a hydrogel is essential for the incorporation of silver nanoparticles with the BI–BO approach. Figure 1 depicts swelling–deswelling cycles of hydrogel sample HGD in distilled water. The observed deswelling in acetone can be attributed to the fact that water, present in the swollen gel matrix, came out because of a strong tendency to form hydrogen bonds with acetone present in the surrounding medium. We performed four such swelling–deswelling cycles and found that the gels maintained their structural integrity throughout the cycles. Moreover, the gels demonstrated higher swelling in the first cycle because of the presence of residual salt within the synthesized gels. This is a common phenomenon and has been reported in a number of studies.[26]

Fabrication and characterization of the hydrogel–silver-nanoparticle composites

As mentioned in the introduction, copolymeric gels, composed of monomers with ionizable groups, have been frequently exploited for the *in situ* formation of silver nanoparticles within the swollen network. However, this approach is not applicable in the case of hydrogels with nonionic repeat units, and so we propose this new BI–BO approach that involves the swelling of a gel in an aqueous solution of silver nanoparticles followed by dewatering of the gel in

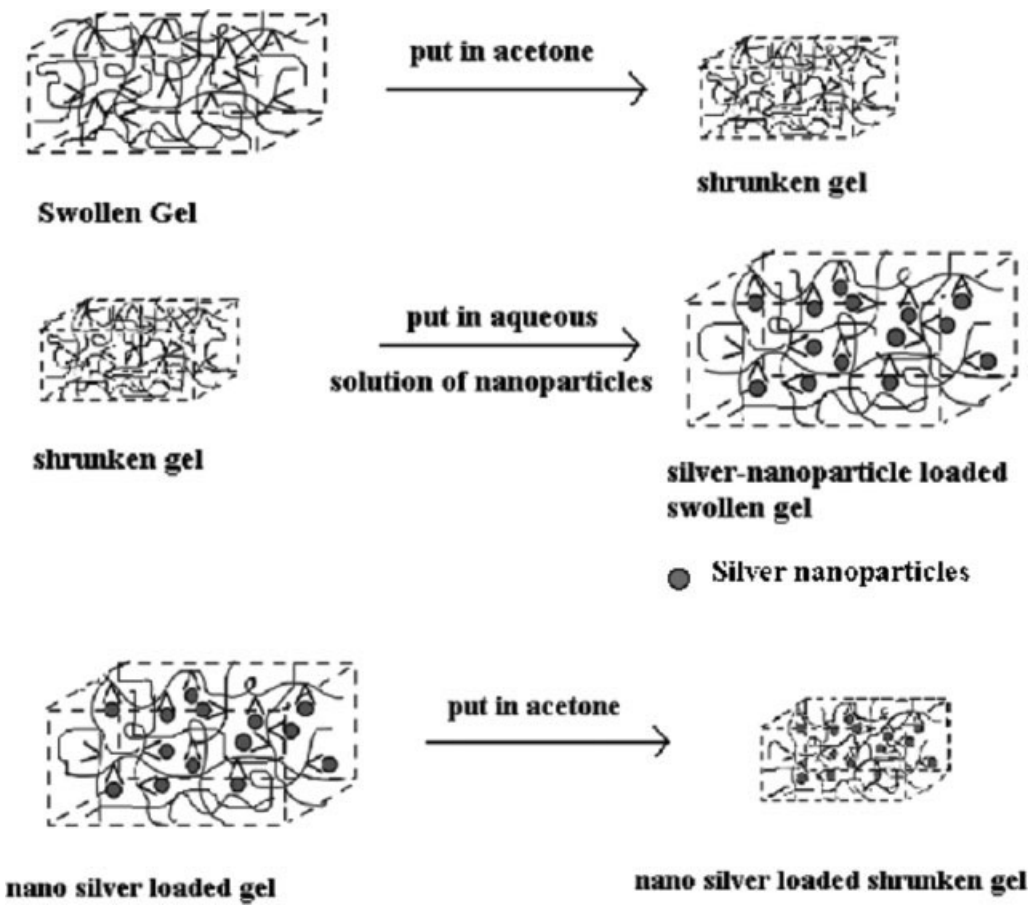

Scheme 1 Formation of silver nanoparticles within the hydrogel.

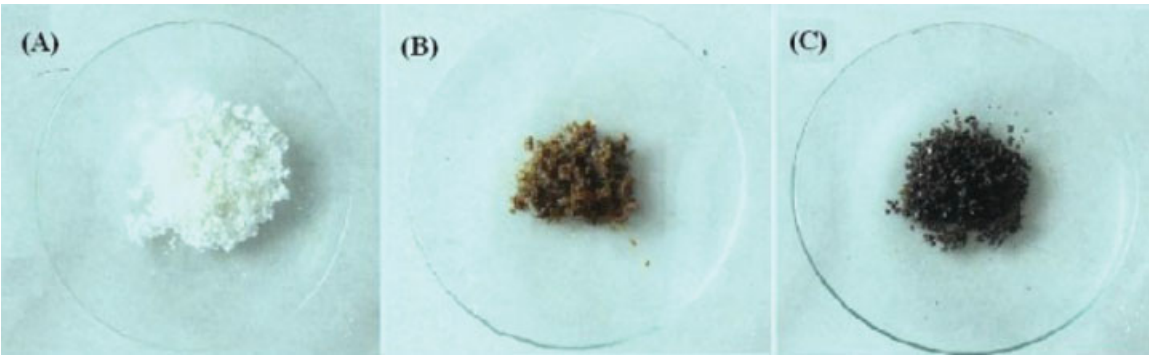

Figure 2 Photograph showing (A) the plain hydrogel (HGA), (B) silver nanocomposites that formed after the first BI–BO cycle, and (C) silver nanocomposites that formed after the second BI–BO cycle. [Color figure can be viewed in the online issue, which is available at www.interscience.wiley.com.]

acetone. The overall mechanism of the proposed BI–BO approach can be described as follows.

When a swollen hydrogel sample is placed in acetone, a drastic volume change occurs because of the expulsion of water molecules, as shown in Scheme 1(A). Then, the shrunken gel is transferred to an aqueous solution of citrate-stabilized silver nanoparticles, in which the hydrogel reswells because of the simultaneous absorption of water molecules and suspended silver nanoparticles [see Scheme 1(B)]. After equilibration of the gel in an aqueous solution of citrate-stabilized silver nanoparticles, it is placed again in acetone, which causes rapid deswelling of the gel network because of the expulsion of water. However, the silver nanoparticles remain stuck inside the gel, probably because of (1) physical entanglement within the macromolecular networks and (2) hydrogen-bonding interactions between the polymer chains and citrate surface of the nanoparticles [see Scheme 1(C)].

The increasing concentration of silver nanoparticles in the gel with breathing-in cycles is well illustrated in Figure 2(A–C), which shows the plain hydrogel and the hydrogel after the first and second BI–BO cycles, respectively. It can be clearly seen that the gel, after undergoing two breathing-in cycles, contained more nanosilver than the sample with one cycle.

The observed increase in the silver content within the hydrogel with the number of BI–BO cycles may be explained as follows. During the breathing-in step, water enters the hydrogel network along with silver nanoparticles. However, when the silver-nanoparticle-containing swollen gel is put into acetone, it undergoes a drastic decrease in volume due to the expulsion of water. However, the silver nanoparticles present within the gel remain inside because of their binding with electron-rich nitrogen and oxygen species of the copolymer network and their physical entanglement with the macromolecular chains. Later on, when the silver-loaded deswelling gel is again placed in an aqueous solution of silver nanoparticles, it begins to swell again because of the absorption of the aqueous medium. During this second breathing-in process, silver nanoparticles again enter the copolymeric hydrogel network and do not come out in the subsequent breathing-out step for reasons similar to those mentioned previously. In this way, each breathing-in step results in the entry of silver nanoparticles into the swelling polymer network along with water.

Different numbers of BI–BO cycles allow us to incorporate more and more silver nanoparticles inside the gel networks. The swelling and deswelling cycles of the plain hydrogel and the hydrogel with different BI–BO cycles (sample HGA) are depicted in Figure 3. The plain hydrogel showed 600% swelling when it was in its swollen form, and after deswelling extensively in an acetone solution, it exhibited a value of 70%. Figure 3 shows the following swelling pattern: hydrogel < third BI–BO cycle

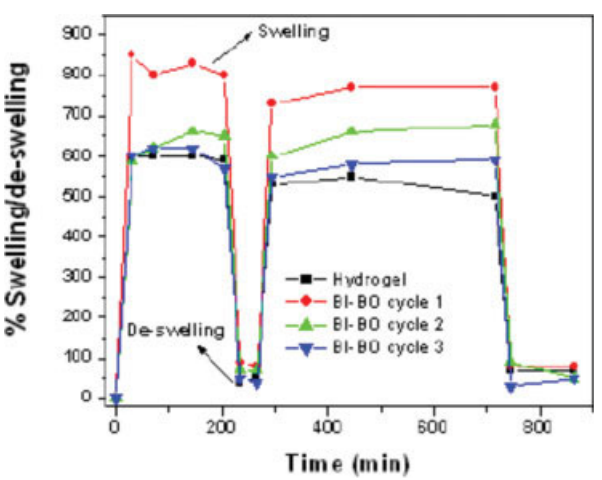

Figure 3 Swelling and deswelling patterns of the plain HGA hydrogel and the HGA hydrogel after undergoing the first, second, and third BI–BO cycles. [Color figure can be viewed in the online issue, which is available at www.interscience.wiley.com.]

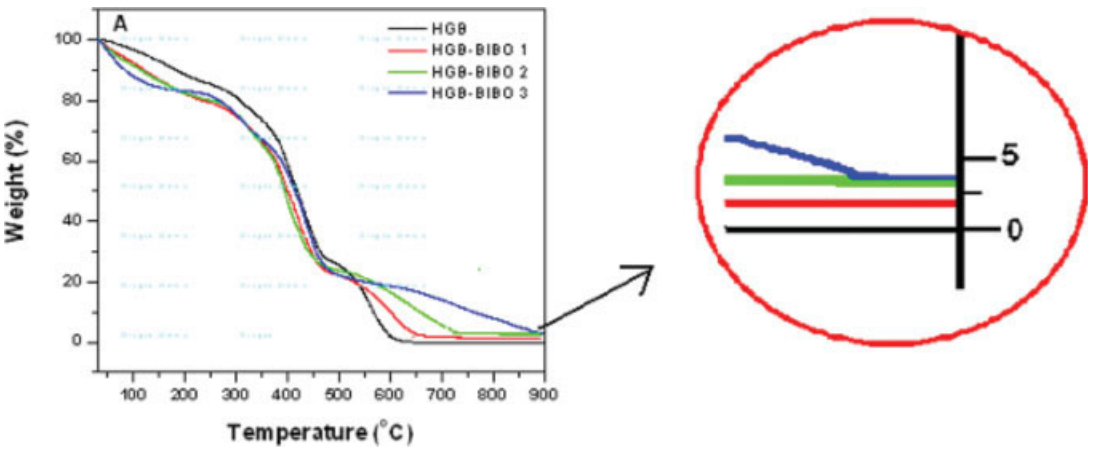

Figure 4 TGA of the plain HGA hydrogel and the HGA hydrogel after undergoing the first, second, and third BI–BO cycles (the magnified area shows the mass percentage remaining at 900°C). [Color figure can be viewed in the online issue, which is available at www.interscience.wiley.com.]

< second BI–BO cycle < first BI–BO cycle. With the first BI–BO cycle, the hydrogel swelling was improved from 600 to ~ 800% because the loaded silver nanoparticles made the hydrogels more hydrophilic in nature, imparting a higher swelling nature to the gels. However, the second and third BI–BO cycles reduced the swelling behavior compared to that after the first cycle because the entrapment of more and more silver nanoparticles inside the gel networks led to a higher crosslink density, which ultimately resulted in a decrease in the swelling properties. The hydrogel after the third BI–BO cycle showed almost the same swelling and deswelling properties as the plain hydrogel.

To further support and provide evidence for our argument that the silver content increases with the number of BI–BO cycles, we carried out thermogravimetric studies of the hydrogels. Thermograms of hydrogel–silver nanocomposites obtained with different cycles and a plain hydrogel (HGA) are presented in Figure 4. All the hydrogels showed three major weight-loss steps. The small weight loss below 100°C had to be due to the loss of water molecules. The second weight loss due to the decomposition of the pendant groups of the hydrogel macromolecular chains was found in the range of 300–450°C for all the hydrogels. However, the third weight loss (i.e., final decomposition temperature) for samples processed with zero, one, two, and three BI–BO cycles was found at 460–600, 500–650, 550–750, and 600–750°C, respectively. The observed increase in the final decomposition temperature with the number of BI–BO cycles may be attributed to the fact that as the number of BI–BO cycles increased, the silver content within the hydrogel networks also increased. As silver has high thermal stability, its presence within the gels enhanced their thermal stability. A close look at the thermograms reveals that the mass percentages remaining at 650°C for the hydrogels processed with one, two, and three BI–BO cycles were nearly 3, 12, and 19%, respectively, thus indicating their enhanced thermal stability. Similarly, the weight percentages remaining at 900°C showed the following order: three cycles (3.1 ± 0.8 wt %) > two cycles (2.7 ± 0.5 wt %) > one cycle (1.8 ± 0.3 wt %; see the magnified portion of Fig. 4). Therefore, it may be claimed that as the number of BI–BO cycles increases, more and more nanosilver enters the hydrogel network, and hence the thermal stability of the resulting gel is also enhanced. Therefore, the enhanced thermal stability of silver-loaded hydrogels prepared with an increasing number of BI–BO cycles is an indication of an increase in the silver content within the hydrogels.

Furthermore, to confirm the amount of nanoparticles loaded into gels with an increase in the number of BI–BO cycles, a UV–vis spectroscopy study was employed. Hydrogel–silver nanoparticles (HGA) obtained with different numbers of BI–BO

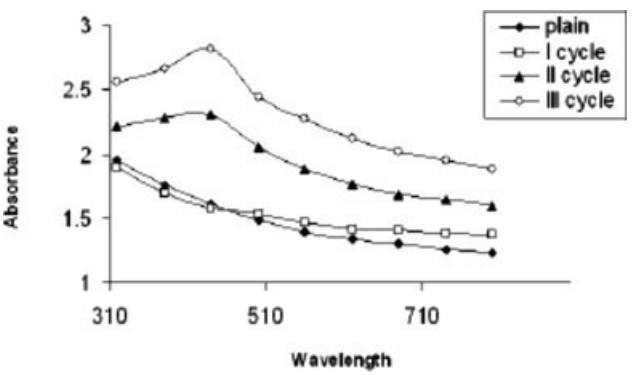

Figure 5 UV–vis spectra of the plain HGA hydrogel and the HGA silver nanocomposites after undergoing the first, second, and third BI–BO cycles.

TABLE II
Amounts of Silver Nanoparticles Loaded into Various Hydrogel Samples Treated with Different BI–BO Cycles

Sample	Amount of silver nanoparticles (μg)				
	I	II	III	IV	V[a]
HGA	112.5	227.5	330.0	444.0	546.5
HGB	100.0	200.0	307.5	396.4	485.3
HGC	90.0	170.0	250.0	338.9	411.4
HGD	60.0	120.0	182.5	235.8	285.8

[a] After the fifth cycle, all samples started to lose their structural integrity.

cycles were soaked for a week in distilled water. The silver nanoparticles released from the plain HGA hydrogels and HGA composites were monitored by absorbance in UV–vis spectra. Figure 5 illustrates higher absorbance for gels with three BI–BO cycles, which directly reflects the presence of higher amounts of particles versus the first and second processed gels.

However, we did not find any peak for the gel that underwent the first BI–BO cycle. This was probably due to the very low concentration of silver nanoparticles released from the gel. It appears that there was a poor loading of silver nanoparticles after the first BI–BO cycle. The figure also depicts the UV–vis spectrum for the plain (i.e., untreated) hydrogel, which does not show any peak at all. Finally, we allowed various samples to go through an increasing number of BI–BO cycles and determined their silver content. The results, as depicted in Table II, clearly reveal that for all samples, the silver content increased with the number of cycles. However, after the fifth cycle, the gels began to disintegrate, and this could be attributed to the presence of additional crosslinks within the gel matrix due to the binding of silver with electron-rich species present in functional groups of macromolecular chains within the network.

To demonstrate the presence of silver nanoparticles within the hydrogel network, TEM images were recorded. For this, finally ground HGB hydrogel nanocomposites were put in distilled water for 7 days, and then their suspension was sonicated. This allowed a few particles to come out of the swollen network. This can probably be attributed to the increased mesh sizes of the swollen network, relaxation of polymeric chain entanglements around the nanoparticles, and finally the decrease in the extent of binding between stabilized silver nanoparticles and nitrogen and oxygen atoms present in the hydrated macromolecular chains. The recorded TEM images are shown in Figures 6 and 7. A close look at these figures reveals not only the presence of released silver nanoparticles but also that of hydrogel–silver nanocomposites. From the size distribution graph [Fig. 7(B)], it can clearly be seen that the average diameter of the silver nanoparticles in the hydrogel comes out to be $\sim$ 12.573 nm.

We also carried out TEM analysis of parent (i.e., original) silver nanoparticles (data not shown), and it was revealed from their particle size distribution curve that their average diameter was nearly 11.5 nm, which was more or less closer to the size of the nanoparticles present in the hydrogel network made with the BI–BO approach. The citrate-stabilized silver nanoparticles apparently did not show any tendency to agglomerate within the hydrogel network. Moreover, it is also equally probable that nitrogen and oxygen atoms present within the copolymeric hydrogel system may also act as binding sites for entrapped nanoparticles, thus resulting in their almost uniform distribution.

A Fourier transform infrared spectrophotometer was used to confirm further the existence of silver

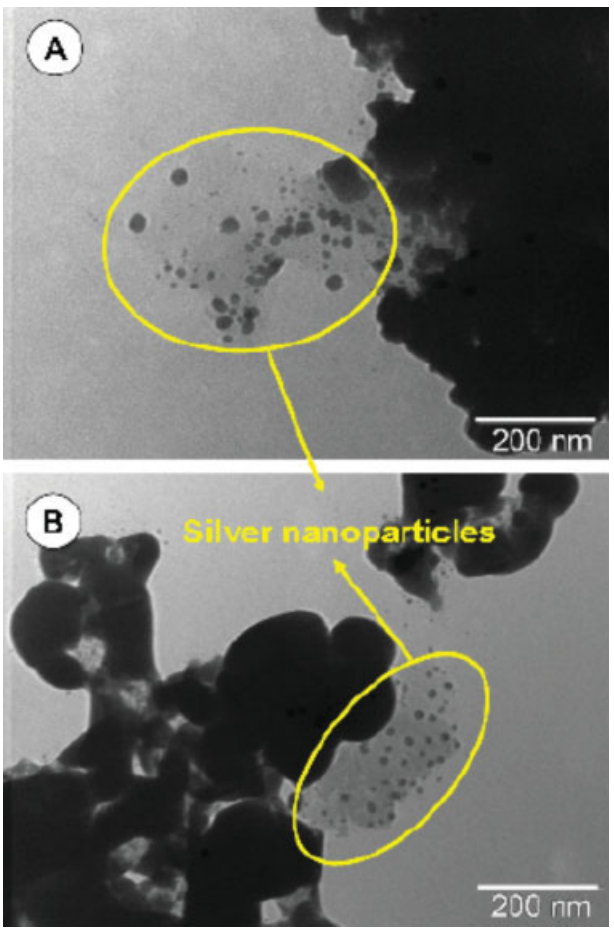

Figure 6 TEM images of nanosilver-loaded HGB hydrogels after undergoing (A) the second BI–BO cycle and (B) the third BI–BO cycle. [Color figure can be viewed in the online issue, which is available at www.interscience.wiley.com.]

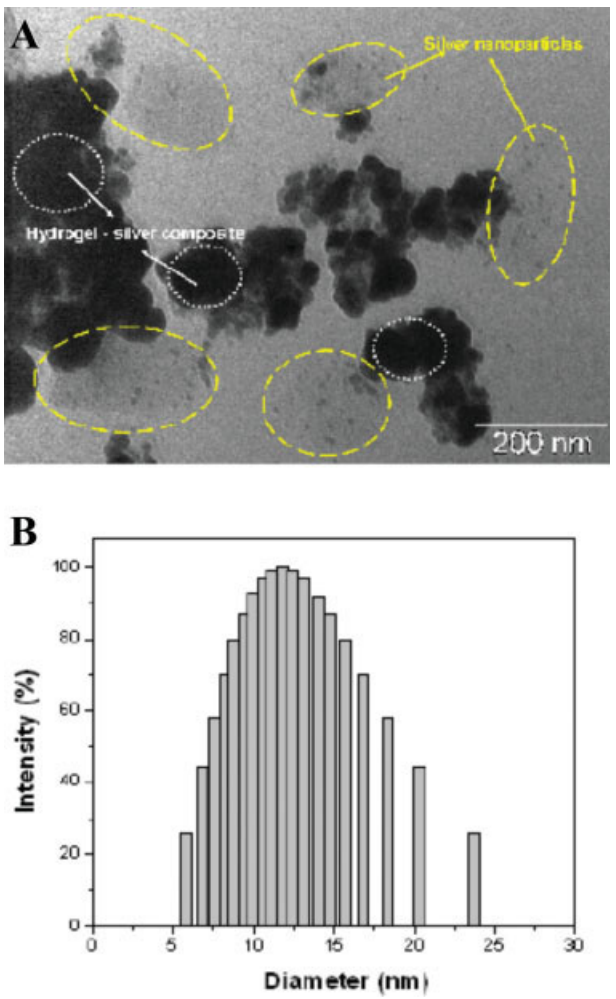

Figure 7 (A) TEM image of the hydrogel–silver nanocomposite (HGB) after undergoing the third BI–BO cycle and (B) size distribution of the silver nanoparticles within the hydrogel. [Color figure can be viewed in the online issue, which is available at www.interscience.wiley.com.]

nanoparticles in the hydrogels. Figure S.1 shows the Fourier transform infrared spectra of the plain hydrogel and hydrogel–silver nanocomposites. C=O stretching can be observed at 1684 cm^{-1} as a sharp peak in the plain sample (b), but it shifted to 1677 cm^{-1} for the gel containing the silver nanoparticles (a). This is evidence that the silver nanoparticles are attached/anchored through the C=O group (of the amide, VP, or both). Similarly, there is also a shift in the NH stretching from 3667 to 3547 cm^{-1}, which is due to the binding of silver nanoparticles with the electron-rich nitrogen species of the copolymeric chain. These peak shifts, mentioned previously, occur because of coordination between the heavy metal atom (silver in this case) and electron-rich groups (oxygen/nitrogen). This causes an increase in the bond length, ultimately leading to a lowering of the frequency.

Antibacterial property of the silver–hydrogel nanocomposites

We aimed at developing silver-nanoparticle-loaded hydrogel composites as antibacterial agents for two main reasons. (1) the hydrogel networks provide excellent stability for silver nanoparticles and can be stored at room temperature, and (2) hydrogels are highly biocompatible in nature. Otherwise, simple polymer-coated or template nanoparticles give stability for a limited time and result in aggregation. By considering these aspects, Mohan et al.[24] demonstrated that the effect of the uptake of silver nanoparticles by *E. coli* depends on the size. Recently, we have shown that the *E. coli* killing ability of hydrogels loaded with silver nanoparticles increases with an increase in the silver content. Furthermore, we anticipate that the current methodology will enable more silver nanoparticles to be loaded, and this is of interest to us. Moreover, the number of BI–BO cycles and the crosslink density of the gel provide feasibility for altering the *E. coli* killing ability. The antibacterial activity of gels loaded with different concentrations of silver nanoparticles has also been evaluated. The detailed results are given next.

Effect of the number of BI–BO cycles on biocidal action

In this method, the silver content in the hydrogel can be increased by an increase in the number of BI–BO cycles. To confirm this, we studied the antibacterial action of 50-mg ground samples of HGB that underwent one, two, or three complete BI–BO cycles. The plain hydrogel was used as a control.

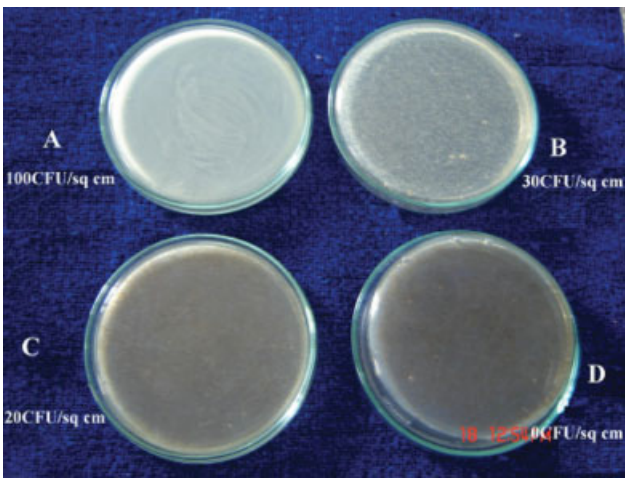

Figure 8 Photograph showing bacterial colonies (A) in a control set and (B–D) in a hydrogel (HGB) after undergoing one, two, or three BI–BO cycles, respectively. [Color figure can be viewed in the online issue, which is available at www.interscience.wiley.com.]

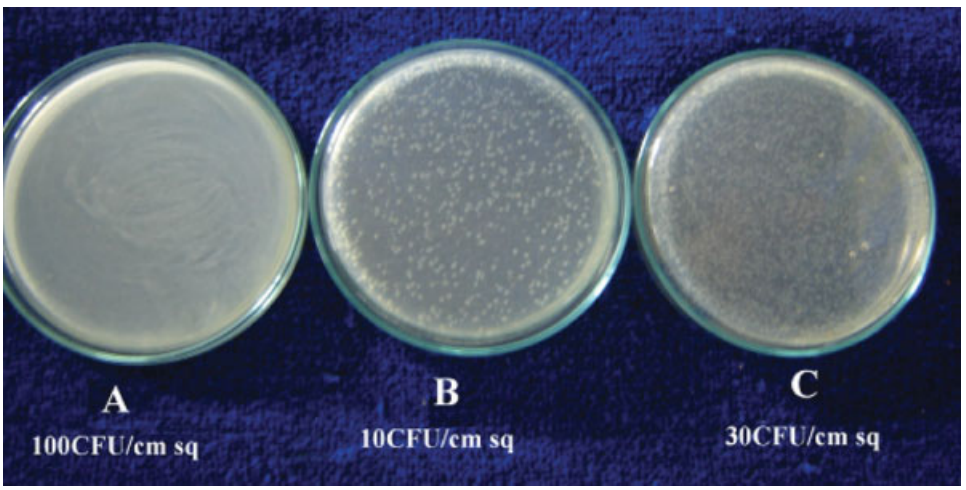

Figure 9 Photograph showing bacterial colonies in (A) a control set, (B) a hydrogel with 0.26 m*M* crosslinker (HGB), and (C) a hydrogel with 0.45 m*M* crosslinker (HGC). Both hydrogels were loaded with one BI–BO cycle. [Color figure can be viewed in the online issue, which is available at www.interscience.wiley.com.]

The results presented in Figure 8 clearly demonstrate that the petri dish containing plain gel particles (HGB) showed the maximum density of bacterial colonies, whereas the petri dishes containing nanosilver-loaded gel particles obtained with one, two, and three BI–BO cycles showed decreasing density of the bacterial colonies. It can be clearly seen from the data displayed that, in comparison with the control set, the number of bacterial colonies was reduced to 30, 20, and nearly 0% for sample HGB with one, two, and three BI–BO cycles, respectively. This may simply be explained by the fact that with an increase in the number of BI–BO cycles, more and more silver nanoparticles are loaded into the gels, and hence the extent of their biocidal action also increases.

Effect of the degree of crosslinking on biocidal action

As mentioned in the previous section, the entrapment of silver nanoparticles in the hydrogel network occurs by hydrogel swelling in an $AgNO_3$ solution (i.e., breathing-in effect). It appears that the silver content in the hydrogel may be a function of its degree of swelling, which, in turn, directly depends on the degree of crosslinking of the polymer network. Thus, we considered hydrogel samples HGB and HGC, which were crosslinked with 0.26 and 0.45 m*M* MBA, loaded them by performing one BI–BO cycle under similar conditions, and finally studied their biocidal action against *E. coli* by taking *E. coli* cultured nutrient agar plates supplemented with 70 mg of ground HGB and HGC. The biocidal action results for the silver–hydrogel

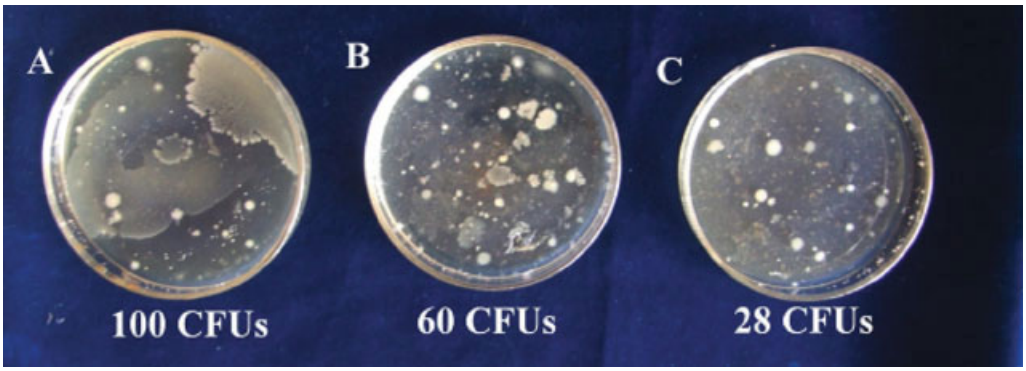

Figure 10 Photograph showing bacterial colonies in (A) a control set, (B) a hydrogel with 0.17×10^{-3} $AgNO_3$ in a nanoparticle solution, and (C) a hydrogel with 0.24×10^{-3} m*M* $AgNO_3$ in a nanoparticle solution. [Color figure can be viewed in the online issue, which is available at www.interscience.wiley.com.]

nanocomposites are illustrated in Figure 9. It can be seen from the displayed data that the bacterial colonies in the petri dishes, containing silver-loaded gels crosslinked with 0.26 and 0.45 m*M* MBA, were reduced to 10 and 30% versus the blank sample. This may be explained by their different swelling capacities. The hydrogel prepared with 0.26 m*M* MBA had a greater degree of swelling in the silver-nanoparticle solution during the breathing-in step, and this allowed more silver nanoparticles to enter the swollen networks. On the other hand, the other sample, crosslinked with 0.45 m*M* MBA, exhibited a lower degree of swelling during the breathing-in step, and this permitted a lower number of silver nanoparticles into the network. Therefore, the degree of crosslinking of a copolymeric gel is a key factor governing the biocidal action of silver–gel composites (antibacterial gel). The other reason is that silver loaded into 0.25 m*M* crosslinked gels is released more easily than silver loaded into 0.45 m*M* crosslinked gels (Fig. S.2), and so silver loaded in 0.25 m*M* crosslinked gels shows more antibacterial activity.

Effect of the $AgNO_3$ concentration on biocidal action

The silver content in the hydrogel (HGB) also increased with the concentration of silver nanoparticles increasing in the solution used in the breathing-in step, which in turn depended on the concentration of the aqueous $AgNO_3$ solution used for the synthesis of the silver nanoparticles. To verify this, 0.17×10^{-3} and 0.24×10^{-3} *M* silver nitrate was dissolved in 50 mL of 1% trisodium citrate (w/v), and the resulting solutions of silver nanoparticles were used in the breathing-in step for loading silver nanoparticles into the swollen gels. The antibacterial results with the resulting nanocomposites are displayed in Figure 10. The obtained results suggest that a 0.17×10^{-3} *M* silver nitrate solution, after being reduced to silver nanoparticles and loaded into a hydrogel, imparts antibacterial properties [see Fig. 10(B)]. On the other hand, a 0.24×10^{-3} *M* $AgNO_3$ solution, when reduced and loaded into a hydrogel, imparts greater biocidal properties, as the composite clearly shows more inhibition of bacterial growth in Figure 10(C). This finding can be attributed to the fact that an $AgNO_3$ solution with a higher concentration (i.e., 0.24×10^{-3} *M*) yields a solution with a greater number of silver nanoparticles on citrate reduction. Therefore, when sample HGB went through the BI–BO cycle with the aforementioned nanosilver solution, more silver nanoparticles were loaded into the hydrogel. Hence, these nanosilver-loaded gels demonstrated greater biocidal action (28 CFU) than the other sample prepared with a 0.17×10^{-3} *M* $AgNO_3$ solution (60 CFU).

Here it is noteworthy to mention that the size and shape of entrapped silver nanoparticles are also significant parameters for controlling their biocidal activity,[27] which in turn depends on the concentration of the $AgNO_3$ solution, the amount of the reducing agent used, the type of stabilizer, the reaction temperature, and so forth.

CONCLUSIONS

From this study, it can be concluded that nonionic hydrogels, that is, poly(acrylamide-*co*-*N*-vinyl-2-pyrrolidone)s, can be highly successful in loading silver nanoparticles with our novel BI–BO approach. These novel nanosystems have been extensively characterized with respect to spectral, thermal, and nanostructural aspects. These nanosilver-loaded hydrogels express good antibacterial activity against *E. coli*. Their antibacterial action depends on the amount of silver nanoparticles within the hydrogel, which can be altered by the number of BI–BO cycles, the amount of $AgNO_3$ in the solution, and the crosslinker in the hydrogels.

The authors are thankful to O. P. Sharma, head of the Department of Chemistry, and Shivani Vishnoi, member of the Department of Biotechnology (Government Model Science College, Jabalpur, India), for their valuable support and the facilities provided for this work.

References

1. Silver, S.; Phung, L. T. Annu Rev Microbiol 1996, 50, 753.
2. Feng, Q. L.; Wu, J.; Chen, G. Q.; Cui, F. Z.; Kim, T. N.; Kim, J. Q. J Biomed Mater Res 2000, 52, 662.
3. Catauro, M.; Raucci, M. G.; De Gaetano, F. D.; Marrotta, A. J Mater Sci: Mater Med 2004, 15, 831.
4. Sondi, I.; Salopek-Sondi, B. J Colloid Interface Sci 2004, 275, 177.
5. Pal, S.; Tak, Y. K.; Song, J. M. Appl Environ Microbiol 2007, 73, 1712.
6. Duran, N.; Marcato, P. D.; De Souza, G. I. H.; Alves, O. L.; Esposito, E. J Nanotechnol 2007, 3, 1.
7. Baker, C.; Pradhan, A.; Pakstis, L.; Pochan, D. J.; Shah, S. I. J Nanosci Nanotechnol 2005, 5, 244.
8. Li, P.; Li, J.; Wu, C.; Wu, Q.; Li, J. Nanotechnology 2005, 16, 1912.
9. Morones, J. R.; Elechiguerra, J. L.; Camacho, A.; Holt, K. J. B. K.; Ramírez, J. T.; Yacaman, M. J. Nanotechnology 2005, 16, 2346.
10. Elechiguerra, J. L.; Burt, J. L.; Morones, J. R.; Camacho-Bragado, A.; Gao, X.; Lara, H. H.; Yacaman, M. J. J Nanobiotechnol 2005, 3, 1.
11. Jain, P.; Pradeep, T. Biotechnol Bioeng 2005, 90, 59.
12. Bosetti, M.; Masse, A.; Tobin, E.; Cannas, M. Biomaterials 2002, 23, 887.
13. Furno, F.; Morley, K. S.; Wong, B.; Sharp, B. L.; Arnold, P. L.; Howdle, S. M.; Bayston, R.; Brown, P. D.; Winship, P. D.; Reid, H. J. J Antimicrobial Chemother 2004, 54, 1019.
14. Lai, K. K.; Fontecchio, S. A. Am J Infect Control 2002, 30, 221.

15. Li, Y.; Leung, P.; Yao, L.; Song, Q. W.; Newton, E. J Hosp Infect 2006, 62, 58.
16. Yu, H.; Yu, X.; Chen, X.; Lu, T.; Zhang, P.; Jing, X. J Appl Polym Sci 2007, 103, 125.
17. Lee, W.; Huang, Y. J Appl Polym Sci 2007, 106, 1992.
18. Mohan, Y. M.; Premkumar, T.; Lee, K.; Geckeler, K. E. Macromol Rapid Commun 2006, 27, 1346.
19. Wang, C.; Flynn, N. T.; Langer, R. Adv Mater 2004, 16, 1074.
20. Zhao, X.; Ding, X.; Deng, Z.; Zheng, Z.; Peng, Y.; Long, X. Macromol Rapid Commun 2005, 26, 1784.
21. Zhang, J.; Xu, S.; Kumacheva, E. J Am Chem Soc 2004, 126, 7908.
22. Lu, Y.; Spyra, P.; Mei, Y.; Ballauff, M.; Pich, A. Macromol Chem Phys 2007, 208, 254.
23. Saravanan, P.; Raju, M. P.; Alam, S. Mater Chem Phys 2007, 103, 278.
24. Mohan, Y. M.; Lee, K.; Premkumar, T.; Geckeler, K. E. Polymer 2007, 48, 158.
25. Thomas, V.; Yallapu, M. M.; Sreedhar, B.; Bajpai, S. K. J Colloid Interface Sci 2007, 315, 389.
26. Bajpai, S. K.; Kalla, K. G.; Bajpai, M. J Appl Polym Sci 2002, 84, 1133.
27. Pal, S.; Tak, Y. K.; Song, J. M. Appl Environ Microbiol 2007, 73, 1712.